Picosecond time-resolved far-infrared experiments on carriers and excitons in GaAs–AlGaAs multiple quantum wells

R. H. M. Groeneveld* and D. Grischkowsky†

IBM T. J. Watson Research Center, Yorktown Heights, New York 10598

Received February 25, 1994; revised manuscript received May 2, 1994

We have investigated the far-infrared (FIR) optical properties and population relaxation dynamics of carriers and excitons in 100-Å GaAs–AlGaAs multiple quantum wells by visible–FIR pump–probe spectroscopy. Our experimental setup is capable of resolving transient changes of the complete complex amplitude transmission coefficient $\Delta t/t$ between 0.3 and 2.3 THz with high sensitivity ($|\Delta t/t| \geq 5 \times 10^{-4}$) and picosecond time resolution. Using picosecond laser pumping pulses to create excitons, we measured the exciton lifetime of 250 ps by monitoring the resulting transient $1s-2p$ exciton absorption (2.0 THz) of a picosecond FIR probing pulse. When free carriers were excited above the quantum-well band edge, we observed not only the decay of the free-carrier population but also the growth of the $1s$ exciton population between 10 and 100 ps. The latter effect is attributed to the relaxation of free carriers into the lowest ($1s$) exciton level.

INTRODUCTION

With the development of picosecond and femtosecond pulsed lasers, it is now possible to study nonequilibrium dynamical processes in semiconductors and other solid-state systems. Until now the available laser sources operated in the visible and infrared parts of the spectrum and did not cover the far infrared (FIR), in which various low-energy excitations are present, such as phonons, magnons, and quasi-particle excitations in superconducting materials as well as electronic transitions in semiconductor quantum structures. With the recent development of picosecond FIR sources, such as those based on laser-driven photoconductive antennas[1] and free-electron lasers, a new class of nonequilibrium phenomena can be studied in the FIR. In this paper we focus on picosecond experiments in which a near-visible laser pump pulse creates an excitation that is monitored by a time-delayed FIR probe pulse. Such experiments have been performed by Nuss *et al.*[2] and Federici *et al.*[3] Here we present a new experimental scheme, using an unamplified Ti:sapphire laser and advanced antenna technology. This scheme allows us to measure the transient change of the complete complex amplitude transmission coefficient ($\Delta t/t$) in the range of 0.3–2.3 THz with a superior detection limit ($|\Delta t/t| \geq 5 \times 10^{-4}$). The unique features of the approach presented are demonstrated in our study of the FIR optical properties and population relaxation dynamics of carriers and excitons in GaAs–AlGaAs multiple quantum wells. Several results are given. We observed the $1s-2p$ internal transition of heavy-hole excitons at 2.0 THz and measured an exciton lifetime of 250 ps. When we excite above the band gap of the quantum wells, we monitor the free-electron population decay and deduce a lifetime of 100–150 ps. In the same measurement the exciton population is seen to increase in time. The latter effect is a direct consequence of the relaxation of free electrons into the lowest ($1s$) exciton state.

EXPERIMENTAL SETUP

The experimental setup is based on a 790–890-nm tunable Ti:sapphire laser, which delivers a beam of 70-fs pulses at a repetition rate of 82 MHz. The beam is split into three beams. Two laser beams drive the optoelectronic receiver and transmitter of FIR pulses that are used as probe pulses. The third beam is used as the laser pump beam. Part of the experimental setup is shown in Fig. 1. We first describe the FIR (terahertz) beam system. Next, we introduce the pump beam and discuss how we measure the pump-induced change of the FIR transmission.

The terahertz beam system[1] is based on photoconductive antennas and has the following features. The photoconductive transmitter antenna is fabricated on semi-insulating GaAs[4] and emits a burst of FIR radiation when irradiated by a short near-visible pulse. The emitted radiation consists of only a few terahertz cycles and therefore covers a broad spectrum. A set of paraboloidal mirrors and silicon lenses images the FIR radiation onto the receiver antenna, which is connected to a current amplifier. The incoming FIR electric field generates a photocurrent through the receiver only when a second, near-visible laser pulse is simultaneously present. The second pulse acts as a gating pulse for the incoming electric field and can be time delayed with respect to the driving transmitter pulse by a computerized translation stage (the receiver delay). Scanning the receiver delay and measuring the photocurrent provide a direct measure of the electric-field strength of the received FIR radiation as a function of time. A Fourier transform of the measured photocurrent yields the amplitude and also the relative phase of each frequency component. In this manner the terahertz beam

0740-3224/94/122502-06$06.00

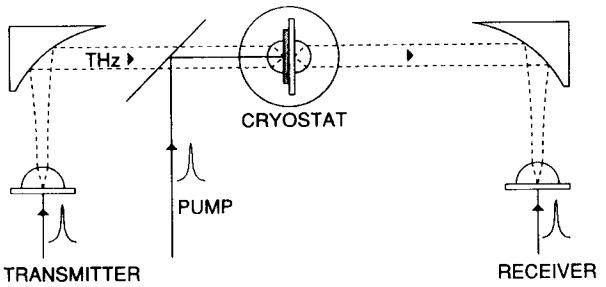

Fig. 1. Part of the experimental setup showing the FIR transmitter and receiver and the cryostat holding the sample that is embedded in a sandwich of quartz lenses. The pump beam is overlapped with the FIR beam.

system has been successfully used for spectroscopy in the frequency range of 0.1–4 THz in various systems[5–7] (1 THz ≡ 33 cm^{-1} ≡ 4.2 meV ≡ 0.3 mm ≡ 50 K). The time delay between the laser pump and FIR probe pulse can be varied by a second, manually driven translation stage (the probe delay). Also, the laser beam's spectral width can be reduced from 20 to 0.5 meV with a 1800-line/mm grating pulse shaper.[8] The pulse duration will increase accordingly from 70 fs to a few picoseconds. The laser pump beam is made collinear with the FIR beam by a beam splitter made from a silicon-on-sapphire wafer.

The sample consists of 50 GaAs wells of 100-Å width, separated by 100-Å barriers of $Al_xGa_{1-x}As$ ($x = 0.33$). The quantum wells are grown on a 500-μm-thick semi-insulating GaAs wafer. The excellent quality of the quantum wells has been verified by photoluminescence emission spectroscopy. We found a photoluminescence emission linewidth of 1.3 meV (FWHM) and a Stokes shift of 1.7 meV. The sample is mounted onto a crystalline sapphire plate that is thermally anchored to the cold finger of a closed-cycle helium cryostat. The temperature of the sample is estimated to be 15 K. On each side of the sample–sapphire sandwich, a quartz lens is mounted. The quartz lenses focus the FIR probe and near-visible pump beams to spot diameters (FWHM of the intensity) of 0.17 and 0.28 mm, respectively.

The time-resolved measurement for a single and fixed time delay between pump and probe pulses consists of two scans of the receiver delay. The two scans are called the main (M) and the difference (D) scan, respectively. We obtain the M scan by placing a chopper in the FIR beam, blocking the pump beam, and scanning the receiver delay line while measuring the photocurrent at the receiver with a lock-in amplifier. The M scan thus represents the transmitted FIR radiation through sample and optics. For the D scan, we switch off the chopper in the FIR beam while letting the beam pass through. A chopper in the pump beam is switched on. Measuring the photocurrent yields the difference of the transmitted FIR radiation with and without the presence of the pump beam. The quotient of the D and M spectra yields the desired change of the amplitude transmission coefficient as a function of the FIR frequency for a particular time delay between the pump and probe pulses. A typical measurement of the M and D scans is shown in Fig. 2 together with the spectra of the M and D scans. It is important to note that the D scan is similar to an inverted M scan. This shows that the attenuation of all frequencies is increased by the pump pulse. The relative amplitude of the D scan with respect to the M scan indicates that the attenuation is of the order of 1%. The deviations from the inverted M-scan shape account for the spectral features to be discussed in detail below. An alternative approach to measuring the amplitude transmission change would be to measure an M scan with the pump on followed by an M scan with the pump off and to determine the difference afterward. It is clear that laser fluctuations on the time scale of the scan duration (several minutes) will now severely limit the performance. The estimated detection limit would be of the order of 5×10^{-3} [approximately the spectral amplitude of the M scan at 3.5–4 THz

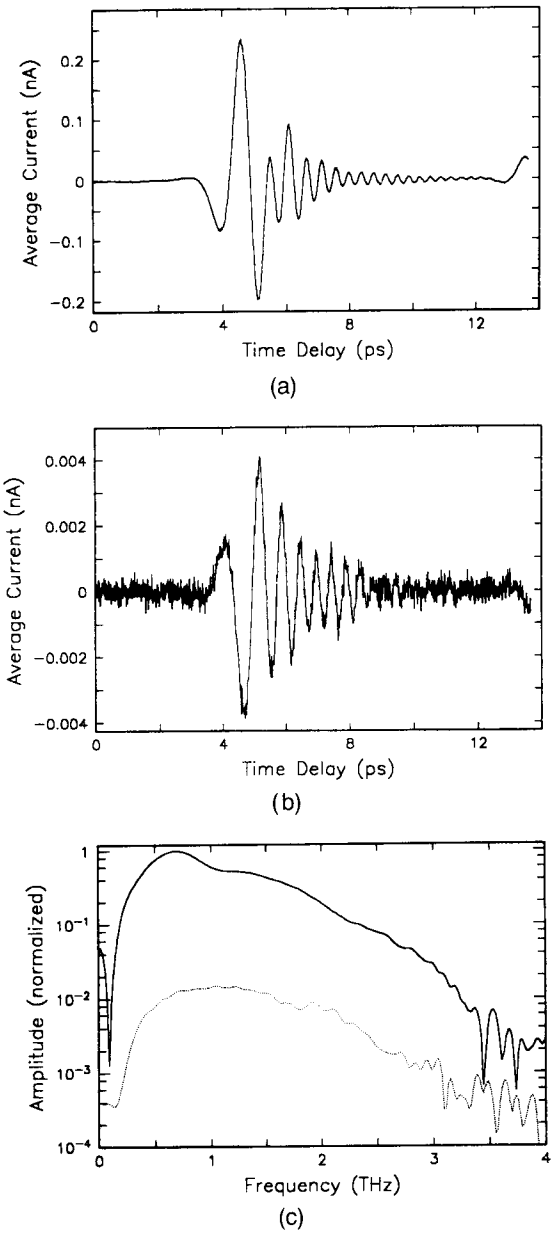

Fig. 2. Measurement of (a) the M scan and (b) the D scan and (c) their spectra (solid curve, M; dotted curve, D). The M scan represents the transmitted FIR electric field through the sample and the optics. The D scan represents the change of the M scan induced by the presence of the pump beam.

in Fig. 2(c)], which is ten times higher than our obtained detection limit (approximately the spectral amplitude of the D scan in the same region).

Several remarks on the experimental method are now made. First, we did not detect a FIR signal from the pump beam alone, which ensured that the method with a single chopper is correct. Second, the frequency resolution of the FIR spectra is determined by the total time width of the M and D scans. The time widths are limited by the secondary received FIR pulse (after 10 ps) that arises from the reflection inside the sample substrate. In our experiments, we obtain a frequency resolution of 100 GHz. The spectra have been numerically smoothed. Third, the operation of the receiver and transmitter does not critically depend on the center wavelength of the laser, which enables us to tune the wavelength of the optical pump pulse over the full laser tuning range. Fourth, it is noted that the spectral contents of the FIR radiation drops at the edges of the spectrum. Hence, the signal-to-noise ratio of the measured amplitude transmission change in these regions will be affected by the loss of signal at the edges. We limit our interpretation of the data to a frequency interval of 0.3–2.3 THz.

MEASUREMENTS AND INTERPRETATION

The measurements have been arranged into three groups according to the photon energy of the pump pulse in relation to the exciton transition of 1.554 eV, as determined by photoluminescence emission. In the three groups the photon energy lies below the exciton transition, at the exciton transition, and above the band gap (1.564 eV) of the quantum well.

When the photon energy of the laser pump beam is tuned below the exciton transition, a peak in the amplitude transmission change $|\Delta t/t|$ is found at 1.1 THz [see Fig. 3(a)]. This peak is independent from the probe delay. When we tune the photon energy from 1.47 up to 1.55 eV, we observe that the strength of the peak reaches a maximum at 1.50 eV, as is shown in Fig. 3(b). The observed energy position of the maximum lies 20 meV below the band gap (1.519 eV) of the semi-insulating GaAs substrate. We have observed this same behavior in a bare semi-insulating GaAs sample.

The above results lead us to the conclusion that the 1.1-THz peak is due to the $1s-2p$ transition of donor-bound electrons that have been photoexcited from filled acceptor states in the substrate. The 1.1-THz peak position matches the absorption peak found in FIR photoconductivity measurements on GaAs.[9] Our observation of the independence from the probe delay time indicates that the donor-bound electrons have a lifetime much larger than the 12-ns repetition time of the laser. Photoluminescence measurements[10] show a lifetime of 0.9 μs, which explains our observation. The measured average acceptor–donor transition energy of 1.50 eV differs, however, from simple estimates that are obtained by subtracting the binding energies of acceptors (30–40 meV) and donors (6 meV) from the band gap.

When the photon energy of the laser pump beam is tuned to the exciton transition at 1.554 eV, we observe the growth of a sharp peak in the amplitude transmission change at 2.0 THz as the probe delay passes zero time delay [see Fig. 4(a)]. The 2.0-THz peak strength decreases on further increase of the probe delay, with a time constant of 250 ps (±20%). The peak disappeared as the pump photon energy was tuned a few milli-electronvolts away on either side from the exciton transition. We interpret the 2.0-THz peak as the absorption of FIR radiation that is due to the $1s-2p$ transition of the photogenerated excitons in the quantum wells. A theoretical estimate[11] yields a value of 1.9 THz, which agrees well with our measured peak position. The characteristic decay time of 250 ps is interpreted as the lifetime of excitons and lies in the 0.2–1-ns range that is given by other measurements.[12,13] Figure 4(b) shows the measured transient phase change.

Our experimental data provide us the opportunity to determine the FIR cross section for the $1s-2p$ exciton transition. The first estimate is based on the measured amplitude transmission change of 0.025 for 50 wells ($|\Delta t/t| = 5 \times 10^{-4}$ per well) under resonant excitation with a 2-meV-bandwidth pump beam. From measured absorption coefficients[14] we deduce a 3% absorption per well and a total light absorption of 78% for 50 wells. We measured a laser fluence of 90 nJ/cm^2 per pulse at the focus. The absorption will create an average exciton density $N_{ex} = 6(1) \times 10^9$ cm^{-2} per well. We find

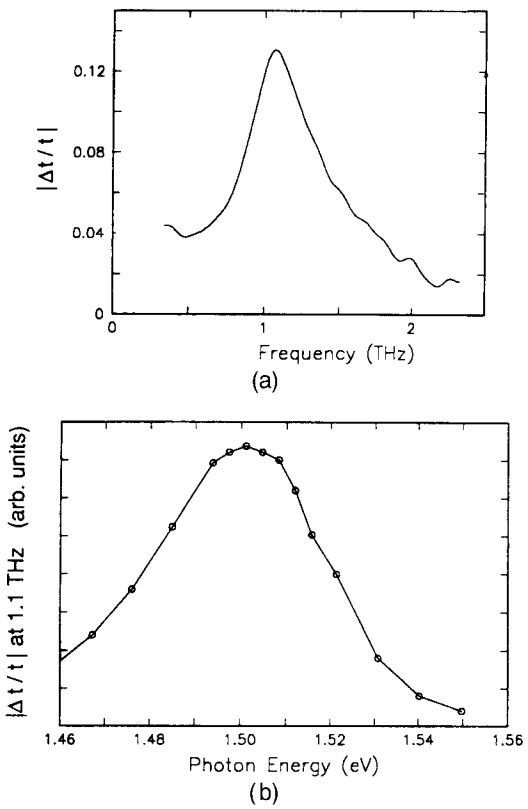

Fig. 3. (a) Measured spectrum of the amplitude transmission change for a pump photon energy of 1.51 eV, which lies below the exciton transition. The transmission decrease at 1.1 THz is due to the FIR absorption by photoexcited donor-bound electrons and is found to be independent of the probe delay time. (b) Strength of the 1.1-THz peak in the measured transmission change as a function of the pump photon energy. Note that the maximum strength lies far below the exciton transition (1.554 eV) and even 20 meV below the band gap (1.519 eV) of the semi-insulating GaAs substrate.

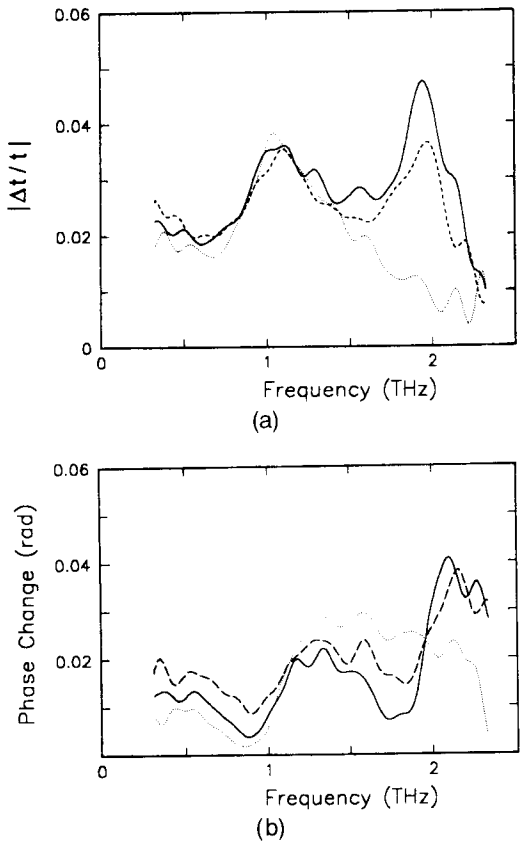

Fig. 4. (a) Measured spectra of the amplitude transmission change for a pump photon energy at the exciton transition and different probe delay times: −10 ps (dotted curve), +10 ps (solid curve), and +100 ps (dashed curve). For the −10-ps curve the probe pulse arrives at the sample 10 ps before the pump pulse. The 2-THz peak is due to absorption by the $1s-2p$ exciton transition. (b) Measured spectra of the phase change.

the FIR cross section for the $1s-2p$ heavy-hole exciton transition to be $\sigma_{1s2p\text{-hh}} = (1/N_{ex})|\Delta t/t| = (42\ \text{Å})^2$. The measured cross section lies close to the value that is found by treating the excitons as an ensemble of hydrogenlike atoms embedded in a background of GaAs. This model leads to[15] $\sigma_{1s2p\text{-hh}} = 2^{19}\pi^2 n^3 \hbar^3 \epsilon_0 \omega\tau/(3^{11}e^2 m_*{}^2 c)$, where $m_* = 0.057m_e$ is the effective reduced exciton mass in GaAs, m_e and e are the electron mass and charge, respectively, ϵ_0 is the vacuum permittivity, c is the speed of light, $n = 3.6$ is the refractive index of GaAs, and $\tau = 1.06$ ps would be the dephasing time of the $1s-2p$ transition if the 0.3-THz measured linewidth of $|\Delta t/t|$ were due to homogeneous broadening. For this case, we find that $\sigma_{1s2p\text{-hh}} = (30\ \text{Å})^2$. The observed linewidth is larger than the 0.14-THz linewidth of the $1s-2p$ exciton transitions in GaAs–AlAs superlattices, as measured by continuous-wave photoinduced FIR absorption.[16] A possible explanation for our large linewidth is that part of the line must be attributed to the $1s-3p$ transition, but this seems unlikely when we consider the small oscillator strength (0.08) of the latter transition. The simplest explanation is that the additional linewidth is due to inhomogeneous broadening as a result of quantum-well variations evidenced by the same 0.3-THz linewidth (1.3 meV) for the photoluminescence emission line. As one can see, the origin of the broadening and whether the line is homogeneously or inhomogeneously broadened remain open questions.

So far we have focused our attention on the exciton absorption itself. We now present data that indicate the interaction between excitons and free electrons. In Fig. 5 we show the pump-delay-dependent part of the amplitude transmission change for different spectral widths of the pump. We obtained the curves by subtracting the measured curve at negative time delay (containing the contribution of donor-bound electrons) from the curves at positive time delay. The pump is centered at the exciton transition. We notice that increasing the spectral width has two effects. First, a low-frequency feature emerges, and, second, the exciton line broadens. The low-frequency feature is interpreted as the absorption by free carriers, which have their absorption peak at zero frequency. Because the band gap of the GaAs substrate lies below the exciton transition, the pump light may excite carriers in the substrate as well, which makes a quantitative interpretation of the data difficult. Lowering the spectral width below 2 meV or decreasing the pump power did not decrease the measured linewidth.

In the last series of measurements, we tuned the pump photon energy to 1.566 eV, above the band gap (1.564 eV) of the quantum wells. In Fig. 6(a) the amplitude transmission changes for different probe delays are plotted. Again, we see that the low-frequency feature rises rapidly when the delay runs from −7 to +10 ps and then decays on the longer time scale (+10 to +100 ps) with a characteristic time of 100–150 ps. The latter value is interpreted as the lifetime of free electrons in the lowest subband of the quantum well. Further, we notice little change of the 1.1-THz peak. However, near the exciton absorption frequency at 2.0 THz, we find a remarkable feature. The absorption at 2.0 THz increases as time increases from 10 to 100 ps. The following dynamical picture emerges. The increase of the absorption is due to an increase of the $1s$ exciton population. The population

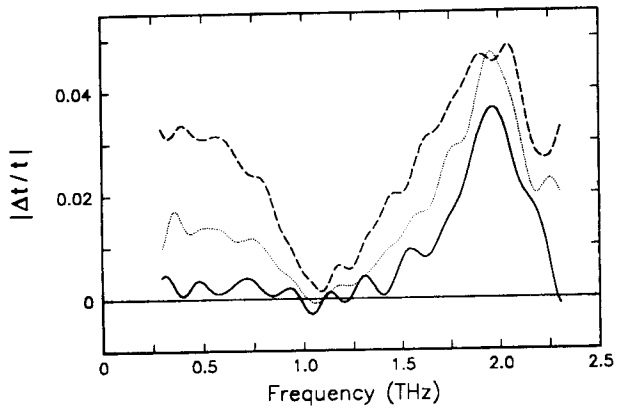

Fig. 5. Measured pump-delay-dependent parts of the spectra of the amplitude transmission change for a pump photon energy at the exciton transition, a probe delay time of +10 ps, and different pump spectral widths: 4 meV (solid curve), 10 meV (dotted curve), and 20 meV (dashed curve). The low-frequency rise is due to free-carrier absorption, and the 2-THz peak is due to the absorption by excitons. The broadening of the exciton peak as the spectral width increases is probably due to exciton–electron interaction.

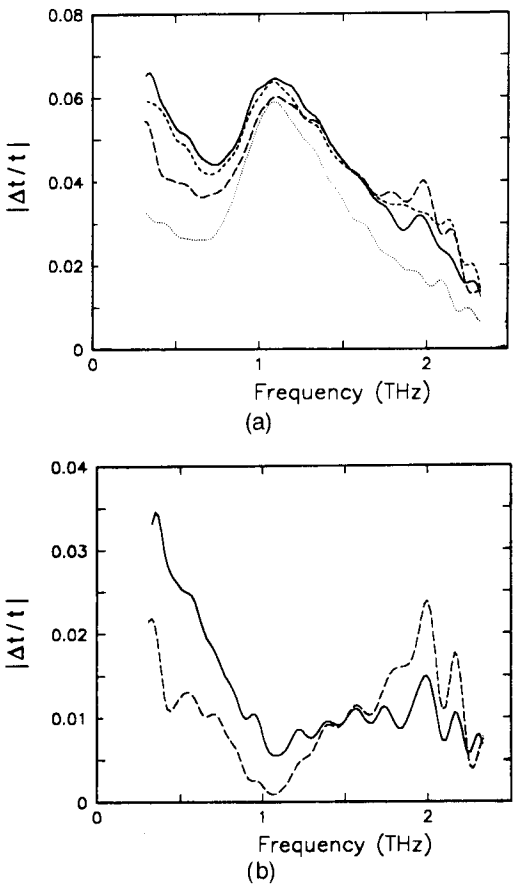

Fig. 6. (a) Measured spectra of the amplitude transmission change for a pump photon energy above the band gap of the quantum well and for different probe delay times: −7 ps (dotted curve), +10 ps (solid curve), +50 ps (short-dashed curve), and +100 ps (long-dashed curve). Below 1 THz the population of free electrons is seen to decay, whereas near 2 THz the exciton population is increasing in time. (b) Pump-delay-dependent part at +10 ps (solid curve) and +100 ps (dashed curve), showing the increased width of the growing exciton absorption.

of free carriers that have been excited into the conduction band not only decays by recombination with holes but also relaxes to the lowest exciton level. The formation of excitons has been studied in more detail by Damen *et al.*[17] by time-resolved luminescence.

In Fig. 6(b) the pump-delay-dependent part is plotted, to show the increased width of the exciton absorption line. Four-wave mixing experiments[18] showed an increase of the homogeneous exciton linewidth when the free-carrier density became larger than 10^9 cm^{-2} per well. Because our estimated excited density of free carriers is of the order of 10^{10} cm^{-2} per well, it is likely that the increased width of the exciton absorption peak is due to exciton–electron interactions.

In conclusion, we have investigated the FIR optical properties and population relaxation dynamics of carriers and excitons in 100-Å GaAs–AlGaAs multiple quantum wells by visible–FIR pump–probe spectroscopy. We measured the exciton lifetime of 250 ps by monitoring the $1s-2p$ exciton absorption in the time domain. When free carriers were excited above the quantum-well band edge, we observed not only the decay of the free-carrier population but also the growth of the 1*s* exciton population between 10 and 100 ps.

ACKNOWLEDGMENTS

We acknowledge the many fruitful discussions with N. Katzenellenbogen and J. Kash and thank H. Chan for the excellent antenna fabrication. R. M. H. Groeneveld thanks the Netherlands America Commission for Educational Exchange for a grant from the Fulbright program.

*Permanent address, University of Nijmegen, Toernooiveld, 6525 ED Nijmegen, The Netherlands.

†Permanent address, School of Electrical and Computer Engineering, Oklahoma State University, Stillwater, Oklahoma 74078.

REFERENCES

1. M. van Exter and D. Grischkowsky, "Characterization of an optoelectronic teraHz beam system," IEEE Trans. Microwave Theory Tech. **38,** 1684 (1990).
2. M. C. Nuss, D. H. Auston, and F. Capasso, "Direct subpicosecond measurement of carrier mobility of photoexcited electrons in gallium arsenide," Phys Rev. Lett. **58,** 2355 (1987).
3. J. F. Federici, B. I. Greene, P. N. Saeta, D. R. Dykaar, F. Sharifi, and R. C. Dynes, "Direct picosecond measurement of photoinduced Cooper-pair breaking in lead," Phys. Rev. B **46,** 11153 (1992).
4. N. Katzenellenbogen and D. Grischkowsky, "Efficient generation of 380 fs pulses of THz radiation by ultrafast laser pulse excitation of a biased metal–semiconductor interface," Appl. Phys. Lett. **58,** 222 (1991).
5. D. Grischkowsky, S. Keiding, M. van Exter, and Ch. Fattinger, "Far-infrared time-domain spectroscopy with terahertz beams of dielectrics and semiconductors," J. Opt. Soc. Am. B **7,** 2006 (1990).
6. H. Harde, S. Keiding, and D. Grischkowsky, "THz commensurate echoes: periodic rephasing of molecular transitions in free-induction decay," Phys. Rev. Lett. **66,** 1834 (1991).
7. N. Katzenellenbogen and D. Grischkowsky, "Electrical characterization to 4 THz of *N*- and *P*-type GaAs using THz time-domain spectroscopy," Appl. Phys. Lett. **61,** 840 (1992).
8. A. M. Weiner, J. P. Heritage, and E. M. Kirschner, "High-resolution femtosecond pulse shaping," J. Opt. Soc. Am. B **5,** 1563 (1988).
9. G. E. Stillman, C. M. Wolfe, and J. O. Dimmock, "Far-infrared photoconductivity in high purity GaAs," in *Semiconductors and Semimetals* (Academic, New York, 1977), Vol. 12, p. 169.
10. X. Liu, L. Samuelson, M.-E. Pistol, M. Gerling, and S. Nilsson, "Donor states in GaAs under hydrostatic pressure," Phys. Rev. B **42,** 11791 (1990).
11. L. C. Andreani and A. Paquarello, "Accurate theory of excitons in GaAs–$Ga_{1-x}Al_xAs$ quantum wells," Phys. Rev. B **42,** 8928 (1990).
12. D. Oberhauser, K. H. Pantke, J. M. Hvam, G. Weimann, and C. Klingshirn, "Exciton scattering in quantum wells at low temperatures," Phys. Rev. B **47,** 6827 (1993).
13. D. Oberhauser, K. H. Pantke, W. Langbein, V. G. Lyssenko, H. Kalt, J. M. Hvam, G. Weimann, and C. Klingshirn, "Coherent and incoherent exciton dynamics in $Al_{1-y}Ga_yAs$/GaAs multiple quantum wells," Phys. Status Solidi B **173,** 53 (1992).
14. Y. Masumoto, M. Matsuura, S. Tarucha, and H. Okamoto, "Direct experimental observation of two-dimensional shrinkage of the exciton wave function in quantum wells," Phys. Rev. B **32,** 4275 (1985).
15. R. Loudon, *The Quantum Theory of Light,* 2nd ed. (Clarendon, Oxford, 1983), p. 44.
16. C. C. Hodge, C. C. Philips, M. S. Skolnick, G. W. Smith, C. R. Whitehouse, P. Dawson, and C. T. Foxon, "Induced

absorption spectroscopic determination of exciton binding energies in type-II GaAs/AlAs superlattices," Phys. Rev. B **41,** 12319 (1990).
17. T. C. Damen, J. Shah, D. Y. Oberli, D. S. Chemla, J. E. Cunningham, and J. M. Kuo, "Dynamics of exciton formation and relaxation in GaAs quantum wells," Phys. Rev. B **42,** 7434 (1990).
18. J. Kuhl, A. Honold, L. Schultheis, and C. W. Tu, "Optical dephasing and orientational relaxation of Wannier excitons and free carriers in GaAs and GaAs/$Al_xGa_{1-x}As$ quantum wells," Festkörperprobleme **29,** 157 (1989).